REGULAR ARTICLE

Atomic shell structure based on inhomogeneity measures of the electron density

K. Wagner · M. Kohout

Abstract A measure of electron density inhomogeneity is proposed based on the distance of function values to the average value within a chosen region. The choice of the examined regions follows the approach of restricted space partitioning with fixed inhomogeneity as the restriction. The integration of electron density over the regions of the partitioning yields discrete distribution of charges, which is analyzed. The resulting functionals depend on the particular definition of distance. Two possibilities are selected for the distance definition, and the functionals are applied to examine the shell structure of the atoms Li to Xe.

Keywords Shell structure · Electron density · Inhomogeneity measure · Space partitioning · Atoms

1 Introduction

Despite all the manifold functionals revealing the shell structure of atoms in real space [1–8], we are convinced that it is still long way to the understanding of the shell formation in coordinate space as well as the impact of the 'physical reality' of this object with respect to the bonding analysis of molecules and crystals. Each of the functionals shows another manifestation of the atomic shell structuring. And each such manifestation is of course the true one, but pointing to different (and sometimes similar) aspects of the underlying physics.

As there is no unequivocal definition of an atomic shell in real space, the notion of 'missing' shell depends, as usually, on the point of view, which is often controlled by the form of the Periodic table of elements, respectively, by the idea of successively filled orbital shells in Hartree-Fock wave function. For instance, the Laplacian of the electron density shows 3 atomic shells for the Ge atom, whereas the one-electron potential (OEP) is able to recover 4 shells [6, 7]. Did density Laplacian fail? Looking at the Cu atom both OEP and the electron localization function (ELF) show 4 shells [1, 6]. However, whereas the former yields 3.2 electrons in the outermost shell, the latter gives appealing 1.1 electrons for the valence shell. Did now OEP fail? We tend to the opinion that this is not the case. The decisive criterion should rather be whether the atomic shells are relevant for the examined problem. Particularly, it should be asked whether the correspondence with the Periodic table is important.

The answer is by no means simple. For instance, Deb and Ghosh proposed to represent the kinetic energy density as a sum of the Weizsäcker term and the kinetic energy density of the homogeneous electron gas weighted by a position-dependent function [9]. This weighting function, which shows atomic shell structure, was fitted by series of Gauss functions. In their work, it was important to get reasonable representation of the weighting function for the conformity with the kinetic energy density. The 'proper' number of atomic shells was irrelevant for their task. Interestingly, the weighting function of Deb and Ghosh is identical with Savin's formulation of ELF [10]. Savin introduced the function for solely different reasons than Deb and Ghosh and, in contrast with the two authors, for ELF the shell structure plays a crucial role [1]. It could be stated, within very simplistic point of view, that the number of atomic shells is possibly not thus important when examining the 'physics' of a functional, but it can be of extreme importance, when striving for relations, or even

K. Wagner (✉) · M. Kohout
Max-Planck-Institut für Chemische Physik fester Stoffe,
Nöthnitzer Str. 40, 01187 Dresden, Germany
e-mail: kati.wagner@cpfs.mpg.de

coincidence, with 'chemical' models (i.e., to achieve proper spatial core-valence separation for chemically meaningful real space descriptors). Whether the 'chemically' appealing real space descriptors are of 'physical' relevance is still an exciting task waiting to be unveiled.

As the proper answer to the above dilemma cannot be faithfully given yet, let us assume here that the conformity between the Periodic table and the spatial shell structure of atoms is an important aspect. Then for the 'ideal' functional the position of the examined element in the Periodic table should clearly determine both, the number of shell descriptors (equating the row number) and the shell populations (following the Aufbau Principle). Actually, there are only very few functionals fulfilling (at least roughly) such requirements, for instance, the electron localizability indicator (ELI) [11–13].

The indicator is based on the approach of ω-restricted space partitioning (ωRSP) [14]. Particularly, the ELI-D follows from space partitioning restricted by fixed fraction of an electron pair (another form of ELI is the ELI-q which is based on ωRSP using fixed electron population as the restriction) [15]. In each so-called micro-cell enclosing the fixed fraction of an electron pair the charge is determined. After rescaling, the ELI-D is a quasi-continuous distribution of values proportional to the charge in the micro-cells (charge needed to form the fixed pair fraction) [15]. ELI-D can be written as $\rho \times \tilde{V}_D$ with the electron density ρ and the pair-volume function $\tilde{V}_D$, which incorporates the local electron pair interactions. Generally, the electron population can be sampled over micro-cells of an ωRSP following any chosen restriction ω. The values of the resulting quasi-continuous distribution can always be given by $\rho \times \tilde{V}_\omega$, with the corresponding volume function $\tilde{V}_\omega$, which need not be connected to electron pair interactions at all. Choosing the volume function $\tilde{V}_\omega$ as suitable electron density functional such that the resulting distribution of charges resembles ELI-D would mean, in certain sense, to approximate the electron pair interaction by an electron density expression. In the following, two measures of electron density inhomogeneity are proposed to serve as the conditions for the ωRSP and the distributions resulting from the charge sampling examined for the atoms Li–Xe.

2 Theory

The nature of quantum mechanics does not admit a direct access to a local interpretation. One of possible concepts to describe a property from a local viewpoint is the ωRSP approach [15]. This approach gives rise to a family of distributions depending on the choice of the so-called control property and the sampling property, respectively. Within this concept, the control property is responsible for the partitioning of the space. The space is subdivided into compact non-overlapping mutually exclusive space filling regions (micro-cells) each enclosing the same (fixed) amount of the control property, thus, yielding a finite number of such regions. After establishing such partitioning, a second quantity is sampled within the regions of the partitioning. The idea behind this partitioning scheme is to 'probe' samples of same 'quality'. This procedure results in a discrete distribution of samples. The sum of this discrete distribution of samples yields the total integral of the sampled property in case that the latter refers to a single-particle function uniquely defined over the whole space (i.e., the definition or parameters are not specific to particular regions).

Similarly to ELI-D, for the functionals proposed in this study, the electron density is chosen as the sampling property, i.e., the sampled quantity is the electronic population in each micro-cell of the space partitioning. Clearly, the sum of all the discrete charges of the distribution recovers the total number of electrons. In contrast with ELI-D, now the space partitioning is controlled by a single-electron property as well (electron pair density in case of ELI-D). The chosen control property is connected with a measure of electron density inhomogeneity. This inhomogeneity measure will be described in the following.

The distance $d_p(f, g)$ between the position $\mathbf{r}$ dependent functions $f(\mathbf{r})$ and $g(\mathbf{r})$ in the region μ_i having the volume V_i can be given by the integral:

$$d_p(f, g) = \sqrt[p]{\int_{\mu_i} |f(\mathbf{r}) - g(\mathbf{r})|^p \mathrm{d}V} \qquad (1)$$

with the positive exponent p. This measure of distance is defined in the space $L_p(\mu_i)$ of functions integrable with p-th power over μ_i.

If g is the average of the function f in the region μ_i, then the resulting distance can be interpreted as an inhomogeneity measure I_p of the function f. For $p = 2$ the distance I_2 is connected with the variance of the function f.

Let us determine the inhomogeneity $I_p(i)$ of the electron density ρ from its average $\bar{\rho}_i$ over the region μ_i:

$$I_p(i) = \sqrt[p]{\int_{\mu_i} |\rho(\mathbf{r}) - \bar{\rho}_i|^p \mathrm{d}V}, \qquad (2)$$

where the average density in μ_i is given by:

$$\bar{\rho}_i = \frac{1}{V_i} \int_{\mu_i} \rho(\mathbf{r}) \mathrm{d}V. \qquad (3)$$

Low inhomogeneity value means that in the examined region the electron density is less varying around the average value than in regions with higher inhomogeneity. Now one

can ask for the electronic population in a region of fixed very low inhomogeneity value. This yields discrete distribution showing what charge is allowed in a region around the examined position to achieve a given inhomogeneity. As mentioned earlier, for the parameter p defining the metric, cf. Eq. 1, any positive number can be taken. In the following, the distances $d_1(\rho, \bar{\rho})$ and $d_2(\rho, \bar{\rho})$ will be used.

2.1 Inhomogeneity measure I_1

The inhomogeneity $I_1(i)$ in $L_1(\mu_i)$ is given by the integral:

$$I_1(i) = \int_{\mu_i} |\rho - \bar{\rho}_i| dV. \tag{4}$$

For regions small enough (micro-cells) the integral can be approximated using the Taylor expansion around the position $\mathbf{a}_i$ (for instance, the center of the micro-cells μ_i):

$$I_1(i) \approx |\rho(\mathbf{a}_i) - \bar{\rho}_i| V_i + \frac{1}{4} |\nabla \rho(\mathbf{a}_i)| V_i^{4/3}. \tag{5}$$

Inserting for the average density $\bar{\rho}_i$ from Eq. 3 with subsequent Taylor expansion finally yields:

$$I_1(i) \approx \frac{1}{4} |\nabla \rho(\mathbf{a}_i)| V_i^{4/3}. \tag{6}$$

For the inhomogeneity I_1 fixed at the value ω_1 the corresponding micro-cell volume over which the integration is performed can be approximately determined:

$$V_i \approx \omega_1^{3/4} \left[\frac{4}{|\nabla \rho(\mathbf{a}_i)|} \right]^{3/4}. \tag{7}$$

The electron population q_i in sufficiently small micro-cell centered around the position $\mathbf{a}_i$ is approximately given by:

$$q_i = \int_{\mu_i} \rho(\mathbf{r}) dV \approx \rho(\mathbf{a}_i) V_i. \tag{8}$$

Replacing for the micro-cell volume V_i from Eq. 7 leads to an expression including the condition of fixed inhomogeneity:

$$q_i \approx \omega_1^{3/4} \rho(\mathbf{a}_i) \left[\frac{4}{|\nabla \rho(\mathbf{a}_i)|} \right]^{3/4}. \tag{9}$$

Of course, the resulting distribution q_i depends on the chosen value of the restriction ω_1. In order to extract the relevant information, which is independent of the restriction magnitude, the charge distribution is rescaled by $\omega_1^{-3/4}$. We define the functional $C_1(i)$ in the $L_1(\mu_i)$ space of the ωRSP micro-cells controlled by fixed infinitesimally small inhomogeneity value ω_1 as the quasi-continuous distribution of rescaled charges (whereas $\{C_1(i)\omega_1^{3/4}\}$ is a discrete set of charges):

$$C_1(i) = \frac{q_i}{\omega_1^{3/4}} \approx \rho(\mathbf{a}_i) \left[\frac{4}{|\nabla \rho(\mathbf{a}_i)|} \right]^{3/4}. \tag{10}$$

The limit after rescaling (continuous function):

$$\tilde{C}_1(\mathbf{r}) = \lim_{\omega \to 0} C_1 = \rho(\mathbf{r}) \tilde{V}_{I_1}(\mathbf{r}) \tag{11}$$

includes the corresponding inhomogeneity I_1 restricted volume function $\tilde{V}_{I_1}$ given by:

$$\tilde{V}_{I_1}(\mathbf{r}) = \left[\frac{4}{|\nabla \rho(\mathbf{r})|} \right]^{3/4}. \tag{12}$$

2.2 Inhomogeneity measure I_2

The distance $d_2(\rho, \bar{\rho})$ in $L_2(\mu_i)$ leads to the inhomogeneity measure for the micro-cell μ_i given by the integral:

$$I_2(i) = \sqrt{\int_{\mu_i} |\rho - \bar{\rho}_i|^2 dV}. \tag{13}$$

The integral can be approximated by the Taylor expansion around the center $\mathbf{a}_i$ of the micro-cell μ_i:

$$\begin{aligned} I_2^2(i) \approx & [\rho(\mathbf{a}_i) - \bar{\rho}_i]^2 V_i \\ & + \frac{1}{2} [\rho(\mathbf{a}_i) - \bar{\rho}_i] |\nabla \rho(\mathbf{a}_i)| V_i^{4/3} \\ & + \frac{1}{12} |\nabla \rho(\mathbf{a}_i)|^2 V_i^{5/3} \\ & + \frac{1}{12} [\rho(\mathbf{a}_i) - \bar{\rho}_i] \nabla^2 \rho(\mathbf{a}_i) V_i^{5/3}. \end{aligned} \tag{14}$$

Inserting for the average density $\bar{\rho}_i$ from Eq. 3 with subsequent Taylor expansion simplifies the above expression to:

$$I_2(i) \approx \sqrt{\frac{1}{12}} |\nabla \rho(\mathbf{a}_i)| V_i^{5/6}. \tag{15}$$

For the inhomogeneity I_2 fixed at value ω_2 the corresponding micro-cell volume can be approximated by:

$$V_i \approx \omega_2^{6/5} \left[\frac{\sqrt{12}}{|\nabla \rho(\mathbf{a}_i)|} \right]^{6/5}. \tag{16}$$

The electron population q_i in a micro-cell μ_i of the ωRSP controlled by the ω_2 restriction is approximately given by (cf. Eqs. 8 and 16):

$$q_i \approx \omega_2^{6/5} \rho(\mathbf{a}_i) \left[\frac{\sqrt{12}}{|\nabla \rho(\mathbf{a}_i)|} \right]^{6/5}. \tag{17}$$

The functional $C_2(i)$ in the $L_2(\mu_i)$ space of the ωRSP micro-cells controlled by fixed infinitesimally small inhomogeneity value ω_2 is the quasi-continuous distribution of rescaled charges:

$$C_2(i) = \frac{q_i}{\omega_2^{6/5}} \approx \rho(\mathbf{a}_i) \left[\frac{\sqrt{12}}{|\nabla\rho(\mathbf{a}_i)|}\right]^{6/5} \tag{18}$$

with the limit after rescaling:

$$\tilde{C}_2(\mathbf{r}) = \rho(\mathbf{r})\,\tilde{V}_{I_2}(\mathbf{r}). \tag{19}$$

The inhomogeneity I_2 restricted volume function $\tilde{V}_{I_2}$ is given by:

$$\tilde{V}_{I_2}(\mathbf{r}) = \left[\frac{\sqrt{12}}{|\nabla\rho(\mathbf{a}_i)|}\right]^{6/5}. \tag{20}$$

2.3 Limiting behavior

Both functionals C_1 and C_2 yield quasi-continuous distributions proportional to the charge within the micro-cells of the ωRSP controlled by the fixed inhomogeneity given by the corresponding measures. The limiting behavior of the distributions can be analyzed using the expressions for the limit after rescaling, cf. Eqs. 11 and 19.

The asymptotic behavior for both distributions is controlled by the behavior of the electron density $\lim_{r\to\infty}\sqrt{\rho} = r^\kappa e^{-\lambda r}$, where $\kappa = (Z-N+1)/(\lambda-1)$, $\lambda = \sqrt{-2\mathrm{IP}}$, Z is the nuclear charge, N the number of electrons and IP the first ionization potential, respectively [16]. As λ is positive the distribution $\tilde{C}_1(\mathbf{r})$ will tend to zero for large r:

$$\lim_{r\to\infty}\frac{\rho(r)}{|\nabla\rho(r)|^{3/4}} = \lim_{r\to\infty}\left[\frac{r^\kappa}{e^{\lambda r}}\right]^{1/2}\left|\frac{2\kappa}{r}-2\lambda\right|^{-3/4} = 0, \tag{21}$$

whereas $\tilde{C}_2(\mathbf{r})$ tends to infinity:

$$\lim_{r\to\infty}\frac{\rho(r)}{|\nabla\rho(r)|^{6/5}} = \lim_{r\to\infty}\left[\frac{e^{\lambda r}}{r^\kappa}\right]^{2/5}\left|\frac{2\kappa}{r}-2\lambda\right|^{-6/5} = +\infty. \tag{22}$$

Using Kato's cups condition $\lim_{r\to 0}|\nabla\rho| = 2Z\rho_0$, the behavior of the distributions approaching the nucleus can be determined [17]:

$$\lim_{r\to 0}\frac{\rho(r)}{|\nabla\rho(r)|^{3/4}} = \left[\frac{1}{(2Z)^3}\,\rho_0\right]^{1/4} \tag{23}$$

$$\lim_{r\to 0}\frac{\rho(r)}{|\nabla\rho(r)|^{6/5}} = \left[\frac{1}{(2Z)^6}\,\frac{1}{\rho_0}\right]^{1/5}. \tag{24}$$

Both functionals tend to a fixed value depending on the value of the density at the nucleus.

The distribution $\tilde{C}_1(\mathbf{r})$ is proportional to the inverse of the reduced density gradient $s(\mathbf{r})$ [18, 19, 20] used in the generalized gradient approximations within the density functional theory. For few atoms, the shell structure as resolved by $s(\mathbf{r})$ was discussed in literature [21, 22]. Interestingly, the reduced density gradient is related to the

gradient expansion of the exchange-correlation energy, whereas C_1 is derived from a measure determining the space partitioning.

3 Results and discussion

For the atoms Li to Xe, the wave functions of Clementi and Roetti were used [23]. Calculations of the evaluated properties have been performed with modified version of the program DGrid [24]. DGrid was also used to determine the minima of the functionals and to integrate the spherically averaged electron density.

It should be mentioned that ELI-D used hereinafter is based either on the σ-spin electron density sampled over micro-cells enclosing fixed fraction of $\sigma\sigma$-spin electron pair (Υ_D^α and Υ_D^β for the majority and minority spin, respectively) or the total electron density sampled over micro-cells enclosing fixed fraction of pair of triplet-coupled electrons (in contrast to triplet ELI-D, where the triplet-coupled electrons are sampled as well).

Due to the sampling of the electron density (total, respectively spin-dependent) over the micro-cells of the ωRSP, the functional form of both C_1 and C_2 is the same as the one for ELI-D and can be generally expressed as the product $\rho \times \tilde{V}_\omega$. The individual functionals are based on different prescriptions for the space partitioning which is reflected, within the limit after rescaling, by specific ω-restricted volume functions $\tilde{V}_\omega(\mathbf{r})$.

Figure 1 compares the inhomogeneity-restricted volume functions $\tilde{V}_{I_1}$ and $\tilde{V}_{I_2}$ with the pair-volume function $\tilde{V}_D$ (triplet-coupled electrons) for the Xe atom. Within the distance up to 0.5 bohr from the nucleus $\tilde{V}_{I_1}$ resembles the pair-volume function better than the volume function $\tilde{V}_{I_2}$. The resemblance is meant in relative fashion as on logarithmic scale the difference equals the ratio logarithm. The relative viewpoint is more suitable because the volume functions influence the corresponding functionals in multiplicative way. In the medium range from 0.5 bohr up to 1.5 bohr from the nucleus both volume functions $\tilde{V}_{I_1}$ and $\tilde{V}_{I_2}$ mimic the pair-volume function in similar manner. Thus, in this range the charge sampling functionals C_1 and C_2 can be expected to behave like ELI-D. For distances from the nucleus larger than 2 bohr, the inhomogeneity-restricted volume functions start to deviate from the pair-volume function, with $\tilde{V}_{I_1}$ below and $\tilde{V}_{I_2}$ above the $\tilde{V}_D$ values. With increasing distances from the nucleus the increase in deviation is much less pronounced for $\tilde{V}_{I_1}$ than for $\tilde{V}_{I_2}$.

Figure 2 shows the distributions C_1, C_2 and ELI-D for the Xe atom. All data were computed from total electron density. C_1 resembles qualitatively the ELI-D distribution over the whole radius range, while for C_2 certain
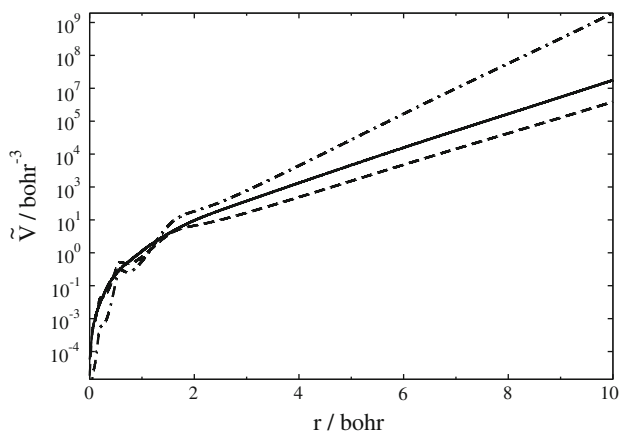
Fig. 1 Volume functions for the Xe atom. *Solid line* pair-volume function $\tilde{V}_D$, *dashed line* volume function for $\tilde{V}_{I_1}$, *dash dotted line* volume function $\tilde{V}_{I_2}$
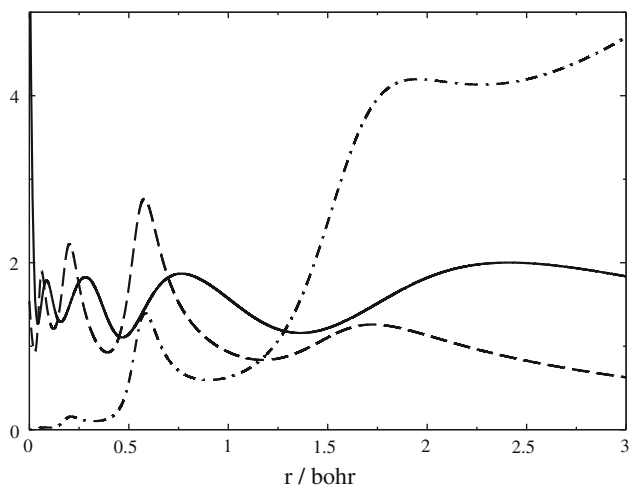

Fig. 2 Charge sampling functionals for the Xe atom. All data were computed from total electron density. *Solid line* ELI-D, *dashed line* C_1, *dash dotted line* C_2

resemblance is given only within a medium range of 0.5–1.5 bohr. This is due to the insufficient resemblance of the volume function $\tilde{V}_{I_2}$ to the pair-volume function. Instead, $\tilde{V}_{I_1}$ matches $\tilde{V}_D$ up to 2 bohr almost perfectly and thus, within this radial range the resulting functionals are alike.

C_1 and C_2 have been calculated for the atoms Li to Xe. For each distribution, the region from the nucleus to the first minimum was assigned to the first shell. Correspondingly, the regions between successive minima were assigned to the higher shells. The radius of the last shell is of course at infinity as the atom extends over the whole space. It turns out that C_2 does not show the expected number of shells for the majority of atoms. Thus, C_2 is not able to represent the shell structure as expected from the Periodic table due to the inadequate behavior of the volume

Table 1 C_1 shell radii and electron populations

Atom	q^K	r^K	q^L	r^L	q^M	r^M	q^N	r^N	q^O
³Li (²S)	1.9	1.3132	1.1	–	–	–	–	–	–
⁴Be (¹S)	1.9	0.8156	2.1	–	–	–	–	–	–
⁵B (²P)	1.9	0.5824	3.1	–	–	–	–	–	–
⁶C (³P)	1.8	0.4436	4.2	–	–	–	–	–	–
⁷N (⁴S)	1.8	0.3532	5.2	–	–	–	–	–	–
⁸O (³P)	1.7	0.2914	6.3	–	–	–	–	–	–
⁹F (²P)	1.7	0.2458	7.3	–	–	–	–	–	–
¹⁰Ne (¹S)	1.7	0.2109	8.3	–	–	–	–	–	–
¹¹Na (²S)	1.6	0.1845	8.3	1.9130	1.1	–	–	–	–
¹²Mg (¹S)	1.6	0.1639	8.2	1.4142	2.2	–	–	–	–
¹³Al (²P)	1.6	0.1473	8.1	1.1626	3.3	–	–	–	–
¹⁴Si (³P)	1.6	0.1335	8.1	0.9844	4.4	–	–	–	–
¹⁵P (⁴S)	1.5	0.1220	8.0	0.8521	5.5	–	–	–	–
¹⁶S (³P)	1.5	0.1139	8.0	0.7510	6.5	–	–	–	–
¹⁷Cl (²P)	1.5	0.1038	7.9	0.6701	7.6	–	–	–	–
¹⁸Ar (¹S)	1.5	0.0965	7.9	0.6045	8.6	–	–	–	–
¹⁹K (²S)	1.5	0.0901	7.9	0.5502	8.6	2.8049	1.1	–	–
²⁰Ca (¹S)	1.5	0.0846	7.8	0.5051	8.4	2.1715	2.3	–	–
²¹Sc (²D)	1.4	0.0797	7.8	0.4671	9.2	2.0248	2.5	–	–
²²Ti (³F)	1.4	0.0754	7.8	0.4338	10.2	1.9507	2.6	–	–
²³V (⁴F)	1.4	0.0715	7.8	0.4046	11.2	1.8847	2.7	–	–
²⁴Cr (⁷S)	1.4	0.0680	7.7	0.3789	13.3	2.2216	1.6	–	–
²⁵Mn (⁶S)	1.4	0.0649	7.7	0.3557	13.2	1.7933	2.7	–	–
²⁶Fe (⁵D)	1.4	0.0620	7.7	0.3351	14.2	1.7444	2.7	–	–
²⁷Co (⁴F)	1.4	0.0592	7.7	0.3170	15.2	1.7069	2.7	–	–
²⁸Ni (³F)	1.4	0.0569	7.6	0.2996	16.3	1.6742	2.7	–	–
²⁹Cu (²S)	1.4	0.0547	7.6	0.2844	20.0	–	–	–	–
³⁰Zn (¹S)	1.4	0.0527	7.6	0.2703	18.4	1.6247	2.6	–	–
³¹Ga (²P)	1.4	0.0507	7.6	0.2575	18.3	1.3908	3.8	–	–
³²Ge (³P)	1.4	0.0489	7.5	0.2458	18.1	1.2246	5.0	–	–
³³As (⁴S)	1.4	0.0472	7.5	0.2351	18.0	1.1023	6.1	–	–
³⁴Se (³P)	1.4	0.0456	7.5	0.2250	18.0	1.0107	7.2	–	–
³⁵Br (²P)	1.4	0.0441	7.5	0.2161	17.8	0.9274	8.3	–	–
³⁶Kr (¹S)	1.4	0.0427	7.5	0.2077	17.8	0.8604	9.4	–	–
³⁷Rb (²S)	1.3	0.0413	7.5	0.1999	17.7	0.8064	9.4	3.2178	1.1
³⁸Sr (¹S)	1.3	0.0401	7.4	0.1927	17.7	0.7580	9.2	2.5404	2.3
³⁹Y (²D)	1.3	0.0389	7.4	0.1860	17.7	0.7195	9.8	2.3514	2.8
⁴⁰Zr (⁵F)	1.3	0.0378	7.4	0.1797	17.7	0.6853	11.4	2.5358	2.1
⁴¹Nb (⁶D)	1.3	0.0367	7.4	0.1739	17.7	0.6525	14.6	–	–
⁴²Mo (⁷S)	1.3	0.0357	7.4	0.1684	17.7	0.6229	15.6	–	–
⁴³Tc (⁶S)	1.3	0.0348	7.4	0.1632	17.6	0.5940	14.1	2.3306	2.5
⁴⁴Ru (⁵F)	1.3	0.0339	7.4	0.1583	17.6	0.5694	17.7	–	–
⁴⁵Rh (⁴F)	1.3	0.0331	7.4	0.1538	17.6	0.5460	18.7	–	–
⁴⁶Pd (¹S)	1.3	0.0323	7.4	0.1494	17.6	0.5247	19.7	–	–
⁴⁷Ag (²S)	1.3	0.0315	7.4	0.1453	17.6	0.5039	20.8	–	–
⁴⁸Cd (¹S)	1.3	0.0307	7.4	0.1417	17.5	0.4855	21.8	–	–
⁴⁹In (²P)	1.3	0.0300	7.4	0.1377	17.5	0.4664	19.4	1.8940	3.5
⁵⁰Sn (³P)	1.3	0.0294	7.4	0.1342	17.5	0.4497	19.0	1.6454	4.9
⁵¹Sb (⁴P)	1.3	0.0287	7.4	0.1309	17.4	0.4341	18.8	1.4794	6.2
⁵²Te (³P)	1.3	0.0281	7.4	0.1277	17.4	0.4196	18.6	1.3581	7.4
⁵³I (²P)	1.3	0.0275	7.3	0.1246	17.4	0.4060	18.4	1.2598	8.6
⁵⁴Xe (¹S)	1.3	0.0269	7.3	0.1217	17.3	0.3932	18.2	1.1763	9.8

q^K, electronic charge in the K shell; r^K, radius of the K shell (in bohr)

function $\tilde{V}_{I_2}$ when compared to the pair-volume function $\tilde{V}_D$, irrespectively whether the total or spin-dependent electron density is sampled. In contrast, the C_1 distribution reflects the 'correct' atomic shell structure by proper number of extrema owing to the suitable behavior of the volume function $\tilde{V}_{I_1}$ when compared to the pair-volume function.

In Table 1, the shell structure based on C_1 using the total density is shown. C_1 reveals the expected number of shells for all atoms, except Cu, Nb, Mo, Ru, Rh, Cd and Ag. The Aufbau Principle demands 2, 8, 18 and 18 electrons for the consecutively fully occupied shells. The inspection of Table 1 shows that the deviations from the Aufbau Principle do not exceed 0.7 electrons for the first three shells, respectively 1.4 and 1.8 for the fourth and fifth shell. In general, the occupation of the inner shells is underestimated. This tendency becomes more pronounced for heavier atoms. The electronic population of the valence shells deviates from the 'ideal' occupation up to 0.3 for the first period. This deviation increases from 0.6 to 1.4 for the second and third period and reaches its maximum for Xe by an excess of 1.8 electrons with respect to the 'ideal' occupation of the valence shell.

In case of separate spin channels, cf. Tables 2 and 3, nearly all calculated atoms show the number of shells in accordance with the Aufbau Principle. However, for the atoms Cr, Nb, Mo, Ru, Rh, and Cd, respectively, the expected outermost shell was missing for the majority spin channel. Interestingly, for the Tc atom the 5th shell is formed by C_1 for the minority spin channel.

Comparing the spin-resolved results to the ones obtained for C_1 based on total density, cf. Table 1, some remarkable differences appear. For the Cr atom, the 4th shell is visible now (occupied by 1.6 electrons). On the contrary, for Cu and Ag the expected outermost shells are no more marked by separate C_1 maximum. Such incongruities may occur because the condition for C_1 extremum is very sensitive to the relationship between the electron density, its gradient and Laplacian.

4 Conclusions

The concept of ω-restricted space partitioning offers a systematic approach for the design of new distributions. This approach was already used for ELI-D, which is based on the sampling of electron density in micro-cells enclosing fixed fraction of same-spin electron pair. Two distributions, based on sampling of the electron density, now in micro-cells of fixed inhomogeneity, were analyzed. The inhomogeneity measure, which defines the volume of the micro-cells, is given by the distance of function values to its average within the micro-cell and depends on the choice

Table 2 C_1 shell radii and electron populations for the majority spin component

Atom	q^K	r^K	q^L	r^L	q^M	r^M	q^N	r^N	q^O
^{3}Li (^{2}S)	1.0	1.1822	1.0	–	–	–	–	–	–
^{4}Be (^{1}S)	0.9	0.8157	1.1	–	–	–	–	–	–
^{5}B (^{2}P)	0.9	0.5532	2.1	–	–	–	–	–	–
^{6}C (^{3}P)	0.9	0.4062	3.1	–	–	–	–	–	–
^{7}N (^{4}S)	0.8	0.3146	4.2	–	–	–	–	–	–
^{8}O (^{3}P)	0.8	0.2707	4.2	–	–	–	–	–	–
^{9}F (^{2}P)	0.8	0.2372	4.2	–	–	–	–	–	–
^{10}Ne (^{1}S)	0.8	0.2109	4.2	–	–	–	–	–	–
^{11}Na (^{2}S)	0.8	0.1844	4.1	1.7269	1.1	–	–	–	–
^{12}Mg (^{1}S)	0.8	0.1639	4.1	1.4142	1.1	–	–	–	–
^{13}Al (^{2}P)	0.8	0.1471	4.0	1.1351	2.2	–	–	–	–
^{14}Si (^{3}P)	0.8	0.1331	4.0	0.9435	3.2	–	–	–	–
^{15}P (^{4}S)	0.8	0.1213	4.0	0.8063	4.3	–	–	–	–
^{16}S (^{3}P)	0.8	0.1134	4.0	0.7247	4.3	–	–	–	–
^{17}Cl (^{2}P)	0.7	0.1035	3.9	0.6587	4.3	–	–	–	–
^{18}Ar (^{1}S)	0.7	0.0965	3.9	0.6045	4.3	–	–	–	–
^{19}K (^{2}S)	0.7	0.0901	3.9	0.5497	4.2	2.5148	1.1	–	–
^{20}Ca (^{1}S)	0.7	0.0846	3.9	0.5051	4.2	2.1715	1.1	–	–
^{21}Sc (^{2}D)	0.7	0.0797	3.9	0.4632	5.0	2.0457	1.4	–	–
^{22}Ti (^{3}F)	0.7	0.0754	3.9	0.4260	6.0	2.0436	1.4	–	–
^{23}V (^{4}F)	0.7	0.0715	3.8	0.3937	7.1	2.0583	1.4	–	–
^{24}Cr (^{7}S)	0.7	0.0680	3.8	0.3644	10.5	–	–	–	–
^{25}Mn (^{6}S)	0.7	0.0648	3.8	0.3404	9.3	2.1277	1.2	–	–
^{26}Fe (^{5}D)	0.7	0.0620	3.8	0.3236	9.3	2.0067	1.2	–	–
^{27}Co (^{4}F)	0.7	0.0591	3.8	0.3088	9.2	1.8829	1.3	–	–
^{28}Ni (^{3}F)	0.7	0.0569	3.8	0.2945	9.2	1.7905	1.3	–	–
^{29}Cu (^{2}S)	0.7	0.0547	3.8	0.2843	9.1	1.7613	1.4	–	–
^{30}Zn (^{1}S)	0.7	0.0527	3.8	0.2703	9.2	1.6247	1.3	–	–
^{31}Ga (^{2}P)	0.7	0.0507	3.8	0.2574	9.0	1.3367	2.5	–	–
^{32}Ge (^{3}P)	0.7	0.0489	3.8	0.2456	8.9	1.1578	3.6	–	–
^{33}As (^{4}S)	0.7	0.0471	3.8	0.2346	8.8	1.0327	4.7	–	–
^{34}Se (^{3}P)	0.7	0.0455	3.7	0.2247	8.9	0.9710	4.7	–	–
^{35}Br (^{2}2P)	0.7	0.0440	3.7	0.2159	8.9	0.9104	4.7	–	–
^{36}Kr (^{1}S)	0.7	0.0427	3.7	0.2077	8.9	0.8604	4.7	–	–
^{37}Rb (^{2}S)	0.7	0.0413	3.7	0.1999	8.9	0.8055	4.6	2.9087	1.1
^{38}Sr (^{1}S)	0.7	0.0401	3.7	0.1927	8.8	0.7580	4.6	2.5404	1.1
^{39}Y (^{2}D)	0.7	0.0389	3.7	0.1859	8.8	0.7171	5.2	2.3607	1.6
^{40}Zr (^{5}F)	0.7	0.0378	3.7	0.1795	8.8	0.6776	6.6	2.3881	2.2
^{41}Nb (^{6}D)	0.7	0.0367	3.7	0.1735	8.8	0.6421	9.8	–	–
^{42}Mo (^{7}S)	0.7	0.0357	3.7	0.1679	8.8	0.6100	10.9	–	–
^{43}Tc (^{6}S)	0.7	0.0348	3.7	0.1626	8.8	0.5806	10.9	–	–
^{44}Ru (^{5}F)	0.7	0.0339	3.7	0.1580	8.8	0.5615	10.9	–	–
^{45}Rh (^{4}F)	0.7	0.0331	3.7	0.1536	8.8	0.5406	10.9	–	–
^{46}Pd (^{1}S)	0.7	0.0323	3.7	0.1494	8.8	0.5247	9.9	–	–
^{47}Ag (^{2}S)	0.7	0.0315	3.7	0.1453	8.8	0.5035	9.7	2.4247	1.1
^{48}Cd (^{1}S)	0.7	0.0307	3.7	0.1417	8.7	0.4855	10.9	–	–
^{49}In (^{2}P)	0.7	0.0300	3.7	0.1377	8.7	0.4663	9.5	1.7861	2.4
^{50}Sn (^{3}P)	0.7	0.0294	3.7	0.1342	8.7	0.4492	9.3	1.5334	3.7
^{51}Sb (^{4}P)	0.7	0.0287	3.7	0.1308	8.7	0.4333	9.1	1.3713	4.9
^{52}Te (^{3}P)	0.6	0.0281	3.7	0.1276	8.7	0.4190	9.1	1.2983	4.9
^{53}I (^{2}P)	0.6	0.0275	3.7	0.1246	8.7	0.4056	9.1	1.2344	4.9
^{54}Xe (^{1}S)	0.6	0.0269	3.7	0.1217	8.7	0.3932	9.1	1.1763	4.9

q^K, electronic charge in the K shell; r^K, radius of the K shell (in bohr)

Table 3 C_1 shell radii and electron populations for minority spin component

Atom	q^K	r^K	q^L	r^L	q^M	r^M	q^N	r^N	q^O
^{3}Li (^{2}S)	1.0	–	–	–	–	–	–	–	–
^{4}Be (^{1}S)	0.9	0.8157	1.1	–	–	–	–	–	–
^{5}B (^{2}P)	0.9	0.6207	1.1	–	–	–	–	–	–
^{6}C (^{3}P)	0.9	0.5029	1.1	–	–	–	–	–	–
^{7}N (^{4}S)	0.9	0.4233	1.1	–	–	–	–	–	–
^{8}O (^{3}P)	0.9	0.3198	2.1	–	–	–	–	–	–
^{9}F (^{2}P)	0.9	0.2556	3.1	–	–	–	–	–	–
^{10}Ne (^{1}S)	0.8	0.2109	4.2	–	–	–	–	–	–
^{11}Na (^{2}S)	0.8	0.1845	4.2	–	–	–	–	–	–
^{12}Mg (^{1}S)	0.8	0.1639	4.1	1.4142	1.1	–	–	–	–
^{13}Al (^{2}P)	0.8	0.1474	4.1	1.1979	1.1	–	–	–	–
^{14}Si (^{3}P)	0.8	0.1340	4.1	1.0489	1.1	–	–	–	–
^{15}P (^{4}S)	0.8	0.1228	4.1	0.9372	1.1	–	–	–	–
^{16}S (^{3}P)	0.8	0.1145	4.0	0.7881	2.2	–	–	–	–
^{17}Cl (^{2}P)	0.7	0.1041	4.0	0.6834	3.3	–	–	–	–
^{18}Ar (^{1}S)	0.7	0.0965	3.9	0.6045	4.3	–	–	–	–
^{19}K (^{2}S)	0.7	0.0901	3.9	0.5507	4.3	–	–	–	–
^{20}Ca (^{1}S)	0.7	0.0846	3.9	0.5051	4.2	2.1715	1.1	–	–
^{21}Sc (^{2}D)	0.7	0.0797	3.9	0.4713	4.2	2.0153	1.1	–	–
^{22}Ti (^{3}F)	0.7	0.0754	3.9	0.4424	4.2	1.9009	1.1	–	–
^{23}V (^{4}F)	0.7	0.0715	3.9	0.4174	4.3	1.7942	1.1	–	–
^{24}Cr (^{7}S)	0.7	0.0681	3.9	0.3973	4.4	–	–	–	–
^{25}Mn (^{6}S)	0.7	0.0649	3.9	0.3756	4.3	1.6232	1.1	–	–
^{26}Fe (^{5}D)	0.7	0.0620	3.9	0.3492	5.2	1.5926	1.2	–	–
^{27}Co (^{4}F)	0.7	0.0592	3.9	0.3264	6.1	1.5831	1.3	–	–
^{28}Ni (^{3}F)	0.7	0.0570	3.8	0.3052	7.1	1.5836	1.4	–	–
^{29}Cu (^{2}S)	0.7	0.0547	3.8	0.2845	9.5	–	–	–	–
^{30}Zn (^{1}S)	0.7	0.0527	3.8	0.2703	9.2	1.6247	1.3	–	–
^{31}Ga (^{2}P)	0.7	0.0507	3.8	0.2576	9.3	1.4795	1.3	–	–
^{32}Ge (^{3}P)	0.7	0.0489	3.8	0.2460	9.3	1.3633	1.2	–	–
^{33}As (^{4}S)	0.7	0.0472	3.8	0.2355	9.3	1.2688	1.2	–	–
^{34}Se (^{3}P)	0.7	0.0456	3.8	0.2254	9.1	1.0700	2.4	–	–
^{35}Br (^{2}P)	0.7	0.0441	3.7	0.2163	9.0	0.9476	3.6	–	–
^{36}Kr (^{1}S)	0.7	0.0427	3.7	0.2077	8.9	0.8604	4.7	–	–
^{37}Rb (^{2}S)	0.7	0.0413	3.7	0.1999	8.9	0.8073	4.7	–	–
^{38}Sr (^{1}S)	0.7	0.0401	3.7	0.1927	8.8	0.7580	4.6	2.5404	1.1
^{39}Y (^{2}D)	0.7	0.0389	3.7	0.1860	8.8	0.7221	4.6	2.3603	1.2
^{40}Zr (^{5}F)	0.7	0.0378	3.7	0.1799	8.9	0.6941	4.8	–	–
^{41}Nb (^{6}D)	0.7	0.0367	3.7	0.1742	8.9	0.6650	4.8	–	–
^{42}Mo (^{7}S)	0.7	0.0357	3.7	0.1688	8.9	0.6394	4.7	–	–
^{43}Tc (^{6}S)	0.7	0.0348	3.7	0.1637	8.9	0.6116	4.6	1.9494	1.1
^{44}Ru (^{5}F)	0.7	0.0339	3.7	0.1586	8.8	0.5786	6.8	–	–
^{45}Rh (^{4}F)	0.7	0.0331	3.7	0.1540	8.8	0.5519	7.8	–	–
^{46}Pd (^{1}S)	0.7	0.0323	3.7	0.1494	8.8	0.5247	9.9	–	–
^{47}Ag (^{2}S)	0.7	0.0315	3.7	0.1453	8.8	0.5042	9.9	–	–
^{48}Cd (^{1}S)	0.7	0.0307	3.7	0.1417	8.7	0.4855	10.9	–	–
^{49}In (^{2}P)	0.7	0.0300	3.7	0.1377	8.7	0.4667	10.0	2.1974	0.9
^{50}Sn (^{3}P)	0.7	0.0294	3.7	0.1343	8.7	0.4502	10.0	2.0311	0.9

Table 3 continued

Atom	q^K	r^K	q^L	r^L	q^M	r^M	q^N	r^N	q^O
^{51}Sb (^{4}P)	0.7	0.0287	3.7	0.1309	8.7	0.4350	10.1	1.8881	0.9
^{52}Te (^{3}P)	0.6	0.0281	3.7	0.1277	8.7	0.4202	9.5	1.4562	2.4
^{53}I (^{2}P)	0.6	0.0275	3.7	0.1247	8.7	0.4063	9.3	1.2907	3.7
^{54}Xe (^{1}S)	0.6	0.0269	3.7	0.1217	8.7	0.3932	9.1	1.1763	4.9

q^K, electronic charge in the K shell; r^K, radius of the K shell (in bohr)

of appropriate exponential parameter. When the parameter equals 1, the inhomogeneity measure is connected with the absolute value of the deviation from the average over the micro-cell. Then, the procedure yields the distribution C_1, which displays the 'correct' shell structure as expected from the Periodic table for the majority of atoms. C_1 can be computed at any level of theory and applied to experimental densities as well.

The functional form for both, the C_1 distribution and ELI-D, can be expressed as the product of the electron density and a function proportional to the micro-cell volume. In case of ELI-D, the pair-volume function (based on the pair density) reflects, in certain sense, the correlation of electronic motion. The similarity between the pair-volume function and the inhomogeneity-restricted volume function (based exclusively on the electron density and its gradient) opens the possibility to examine how accurate the correlation of electronic motion can locally be described as a function of electron density.

References

1. Kohout M, Savin A (1996) Int J Quantum Chem 60:875–882
2. Schmider HL, Becke AD (2000) J Mol Struct (Theochem) 527:51–61
3. Sen KD, Slamet M, Sahni V (1993) Chem Phys Lett 205:313–316
4. Schmider H, Sagar R, Smith VH Jr (1994) P Indian Acad Sci 106:133–142
5. Kohout M, Savin A, Preuss H (1991) J Chem Phys 95:1928–1942
6. Kohout M (2001) Int J Quantum Chem 83:324–331
7. Shi Z, Boyd RJ (1987) J Chem Phys 88:4375–4377
8. Sagar RP, Ku ACT, Smith VH Jr, Simas AM (1987) J Chem Phys 88:4367–4374
9. Deb BM, Gosh SK (1983) Int J Quantum Chem 13:1–26
10. Savin A, Jepsen O, Flad J, Anderson OK, Preuss H, von Schnering HG (1992) Angew Chem 104:186–188
11. Kohout M, Pernal K, Wagner FR, Grin Y (2004) Theor Chem Acc 112:453–459
12. Kohout M, Pernal K, Wagner FR, Grin Y (2005) Theor Chem Acc 113:287–293
13. Kohout M, Wagner FR, Grin Y (2008) Theor Chem Acc 119:413–420
14. Pendas AM, Kohout M, Blanco MA, Francisco E (2010) Beyond standard charge density topological analyses. In: Gatti C, Macchi P (eds) Modern charge density analyses. Springer, London, in publication

15. Kohout M (2007) Faraday Discuss 135:43–54
16. Hoffmann-Ostenhof M, Hoffmann-Ostenhof T (1977) Phys Rev A 16:1782–1785
17. Kato T (1957) Commun Pur Appl Math 10:151–177
18. Perdew JP, Chevary JA, Vosko SH, Jackson KA, Pederson MR, Singh DJ, Fiolhais C (1992) Phys Rev B 46:6671–6687
19. Perdew JP, Burke K, Ernzerhof M (1996) Phys Rev Lett 77:3865–3868
20. Perdew JP, Ernzerhof M, Zupan A, Burke K (1998) J Chem Phys 108:1522–1531
21. Zupan A, Perdew JP, Burke K, Causa M (1997) Int J Quant Chem 61:835–845
22. Arbuznikov AV, Kaupp M (2007) Chem Phys Lett 440:160–168
23. Clementi E, Roetti C (1974) At Data Nucl Data Tables
24. Kohout M (2009) DGrid, version 4.5. Radebeul